

Self-Assembly of a #-Cyclodextrin Bis-Inclusion Complex Into Highly Crystalline Fiber Network. An Effective Strategy for Null Aggregate Design

Nagaraj Nayak, and Karical Raman Gopidas

J. Phys. Chem. B, **Just Accepted Manuscript** • Publication Date (Web): 03 Sep 2019

Downloaded from pubs.acs.org on September 3, 2019

Just Accepted

“Just Accepted” manuscripts have been peer-reviewed and accepted for publication. They are posted online prior to technical editing, formatting for publication and author proofing. The American Chemical Society provides “Just Accepted” as a service to the research community to expedite the dissemination of scientific material as soon as possible after acceptance. “Just Accepted” manuscripts appear in full in PDF format accompanied by an HTML abstract. “Just Accepted” manuscripts have been fully peer reviewed, but should not be considered the official version of record. They are citable by the Digital Object Identifier (DOI®). “Just Accepted” is an optional service offered to authors. Therefore, the “Just Accepted” Web site may not include all articles that will be published in the journal. After a manuscript is technically edited and formatted, it will be removed from the “Just Accepted” Web site and published as an ASAP article. Note that technical editing may introduce minor changes to the manuscript text and/or graphics which could affect content, and all legal disclaimers and ethical guidelines that apply to the journal pertain. ACS cannot be held responsible for errors or consequences arising from the use of information contained in these “Just Accepted” manuscripts.

1
2
3
4
5
6 **Self-assembly of a β -cyclodextrin Bis-inclusion Complex into Highly Crystalline Fiber**
7
8 **Network. An Effective Strategy for Null Aggregate Design**
9

10
11
12 Nagaraj Nayak and Karical Raman Gopidas*

13
14
15 Photosciences and Photonics Section, Chemical Sciences and Technology Division,
16
17 CSIR-National Institute for Interdisciplinary Science and Technology, Trivandrum 695 019 (India)
18
19
20
21
22
23
24
25
26
27
28
29
30
31
32
33
34
35
36
37
38
39
40
41
42
43
44
45
46
47
48
49
50
51
52
53
54
55
56
57
58
59
60

ABSTRACT: The present work deals with the tight molecular packing of a bis-inclusion complex into rigid, 1-D nanofibers. The bis-adamantane linked anthracene derivative AD-AN-AD readily formed the β -CD bis-inclusion complex, $\beta\text{-CD}\subset\text{AD-AN-AD}\supset\beta\text{-CD}$, which spontaneously assembled into a nanofiber network. WAXS pattern of the dried nanofibers indicated that these are highly crystalline in nature. Spectroscopic data of the aggregate are identical to those of the monomeric species, suggesting that the aggregate is not a regular H- or J-aggregate. We propose that the nanofibers constitute another example of the recently proposed class of “null” aggregates, based on the crystal structure and molecular packing in compound **3** which is the precursor of AD-AN-AD. The molecular packing in **3** actually provides a strategy for the design of null aggregates. We propose that the nanofibers are formed from null aggregates of $\beta\text{-CD}\subset\text{AD-AN-AD}\supset\beta\text{-CD}$, wherein the anthracene moieties are twisted in the range $60\text{-}72^\circ$, and this assignment is in line with the spectroscopic studies and NMR titration experiments.

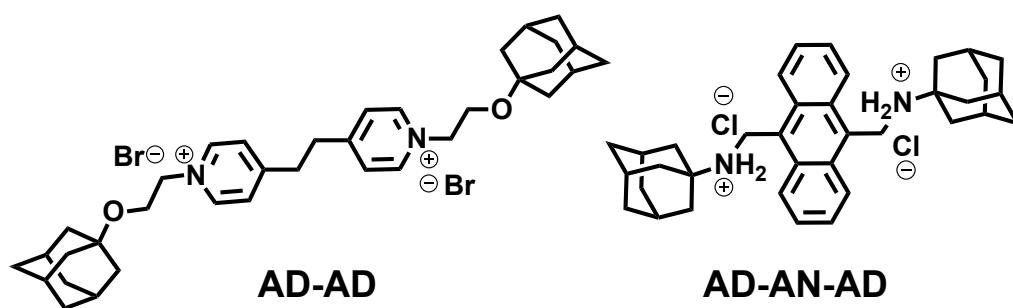
1. INTRODUCTION

Bolaamphiphiles are amphiphilic molecules that contain two polar head groups connected by a hydrophobic linker.¹⁻⁵ Because of their propensity to self-assemble into various morphologies, they are considered as important building blocks for the construction of various nanostructures. For example, bolaamphiphiles are known to self-assemble into spheres,⁶⁻⁹ gels,^{3,10-14} discs,¹⁵⁻¹⁸ vesicles,¹⁹⁻²⁵ helical structures,²⁶⁻²⁹ tubes²⁸⁻³³ etc. Construction of supramolecular amphiphiles and study of their self-assembly into various morphological structures is an important aspect of current supramolecular chemistry.^{2,34-40} Bis-inclusion complexes of cyclodextrins (CD), where the included moieties are present at the two ends of a sufficiently hydrophobic linker unit, can be considered as supramolecular bolaamphiphiles.^{36-37, 41-45} The high water solubility of CDs makes both ends of these bis-inclusion complexes hydrophilic. Although supramolecular amphiphiles are known to self-assemble in to various types of morphologies, bis-inclusion complexes of CDs are known to self-assemble only into vesicles.⁴⁶⁻⁵⁰ In this paper we present self-assembly of a β -CD bis-inclusion complex into crystalline fibers for the first time.

Recently we reported the unusual self-assembly of a β -CD bis-inclusion complex into vesicles capable of encapsulating and releasing drug molecules.⁴⁹ We prepared the molecule AD-AD (Figure 1) which has adamantane (AD) units at both ends. Because of the propensity of AD derivatives to form inclusion complexes with β -CD, the molecule forms the bis-inclusion complex $\beta\text{-CD}\subset\text{AD-AD}\supset\beta\text{-CD}$. We have observed that the $\beta\text{-CD}\subset\text{AD-AD}\supset\beta\text{-CD}$ spontaneously aggregated into vesicles. The self-assembly was unusual because, in all the reported cases of vesicle formation from bis-inclusion complexes, these complexes were identified as supramolecular bola-amphiphiles, with the CD acting as the hydrophilic head group and the alkyl or aryl residue acting as the hydrophobic core. In the case of $\beta\text{-CD}\subset\text{AD-AD}\supset\beta\text{-CD}$, both the end groups and the central 1,2-bis(4-pyridyl)ethane moieties are hydrophilic. The +ve charges on the pyridinium nitrogens of adjacent layers are expected to repel each

1 other and hence the inclusion complex $\beta\text{-CD}\subset\text{AD-AD}\supset\beta\text{-CD}$ was not expected to stack one over the
2 other to give vesicles. However, vesicle formation was observed and confirmed by dynamic light
3 scattering, AFM, SEM and TEM. We also showed that these vesicles could be loaded with the
4 anticancer drug doxorubicin and the loaded drug can be released upon addition of a competitive binding
5 agent such as adamantane carboxylate.⁴⁹
6
7
8
9
10
11

12
13 Herein we report the synthesis and inclusion complexation of AD-AN-AD (Figure 1) in which
14 an anthracene moiety replaces the central 1,2-bis(4-pyridyl)ethane moiety of AD-AD. AD-AN-AD
15 differs from our previous molecule in few respects. The central 1,2-bis(4-pyridyl)ethane moiety is
16 replaced by a more hydrophobic and rigid anthracene unit. The central unit is devoid of any charges, but
17 the two AD moieties at the ends now carry positive charges. These changes have made the end units
18 more hydrophilic and the central units more hydrophobic compared to AD-AD, and the overall length of
19 the molecule is reduced. We observed that AD-AN-AD readily forms the bis-inclusion complex $\beta\text{-CD}\subset\text{AD-AN-AD}\supset\beta\text{-CD}$,
20 which spontaneously self-assembled into highly crystalline fibrous networks.
21 In order to explain the crystalline nature of the fibers and the absence of excitonic coupling in the
22 aggregate, we have invoked the newly introduced concept of “null” aggregates. We propose that $\beta\text{-CD}\subset\text{AD-AN-AD}\supset\beta\text{-CD}$
23 packs one over the other with a twist angle in the range of $60\text{-}72^\circ$ so as to
24 avoid steric hindrance and achieve a $\pi\text{-}\pi$ stacking distance of 3.64 \AA . In this report, details of the
25 inclusion complexation and further self-assembly into fibers are presented along with a discussion of the
26 aggregation process.
27
28
29
30
31
32
33
34
35
36
37
38
39
40
41
42
43
44
45



57 Figure 1. Structures of AD-AD and AD-AN-AD.
58
59
60

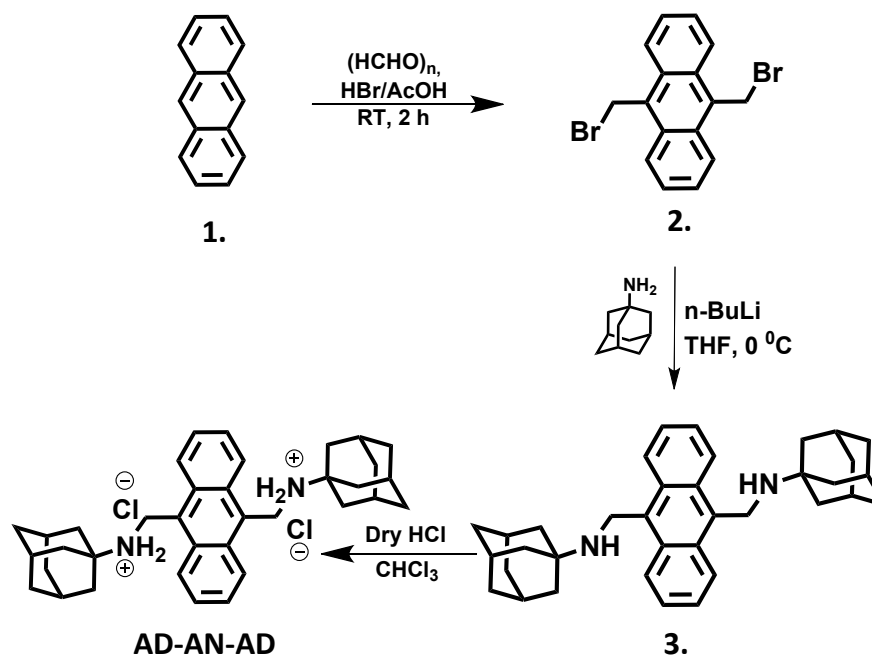
2. METHODS

General Methods. β -CD and all other chemicals were purchased from Aldrich and used as received. The solvents and reagents were dried and purified by standard methods prior to use. Aqueous sample solutions were prepared using double distilled water. The electronic absorption spectra were recorded on a Shimadzu 2401PC UV-VIS-NIR scanning spectrophotometer. ITC data were obtained using microcal iTC 200. The raw data obtained were fitted and analyzed using origin 7.0 software provided along with the instrument. In order to analyze the data, one site (or two identical sites) binding model was assumed and the thermogram was fitted using nonlinear regression procedure.⁵¹ The standard deviations reported for the parameters are those obtained from the fit. All NMR data were recorded in D₂O purchased from Aldrich, using a 500 MHz Bruker Avance DPX spectrometer. AFM measurements were carried out using Bruker multimode 8-HR instrument using micro fabricated TiN cantilever tips (NSG-10) with a resonating frequency of 299 kHz and a spring constant of 20-80 Nm⁻¹ using tapping mode techniques. The samples for AFM were prepared by drop casting the solution on freshly cleaved mica surface and the excess solvent was evaporated. TEM analyses were performed using a FEI-TECNAI T30 G2S-TWIN, 300 kV HRTEM microscope with an accelerating voltage of 100 kV and the samples were prepared by drop casting the solution on a formvar coated copper grid (400 mesh) and evaporating excess solvent. The 2D X-ray measurements were carried out with Xeuss SAXS/WAXS system using a dried film of the sample cast on aluminium foil. Steady-state fluorescence experiments were performed with a SPEX Fluorolog F112X spectrofluorimeter by using optically dilute solutions. Time-resolved fluorescence experiments were performed by using an IBH picosecond single-photon-counting system employing a 375 nm nanoLED excitation source and a Hamamatsu C4878-02 microchannel plate detector. A single crystal of molecule **3** was grown in CHCl₃/CH₃OH solvent

1 mixture and the crystal was analyzed by Saturn 724+ HG single crystal x-ray diffractometer using Mo
2
3
4 K_{α} ($\lambda = 0.71073 \text{ \AA}$) X-rays.
5
6
7
8

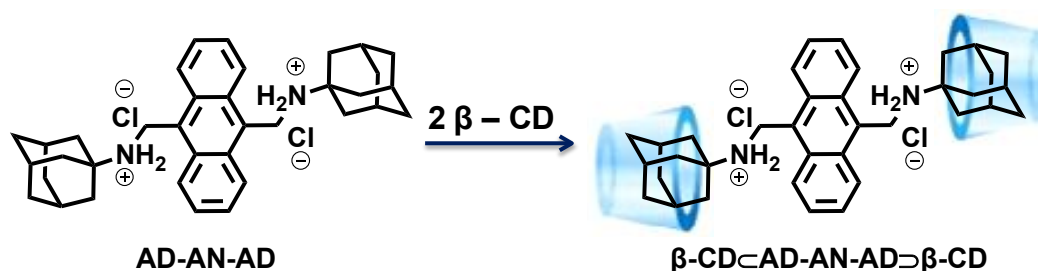
9 3. RESULTS AND DISCUSSION

10
11 **Synthesis and Characterization of AD-AN-AD.** AD-AN-AD was synthesized as shown in
12 Scheme 1. Anthracene was converted into 9,10-bisbromomethylanthracene using paraformaldehyde and
13 HBr in glacial acetic acid.⁵² This was treated with two equivalents of adamantylamine in the presence of
14 n-butyllithium. The bisadamantyl adduct **3** was converted to its hydrochloride salt (AD-AN-AD) by
15 treatment with dry HCl gas. All the intermediates and final products were characterized by ¹H NMR,
16 ¹³C NMR and HRMS techniques [see experimental section and supporting information (Figures S1-S6)
17 for more details]. Structure of the intermediate **3** was also confirmed by single crystal X-ray analysis.
18 AD-AN-AD was found to be sufficiently soluble in aqueous medium because of the two positive
19 charges in the molecule.
20
21
22
23
24
25
26
27
28
29
30
31
32
33
34
35
36
37
38
39
40
41
42
43
44
45
46
47
48
49
50
51
52
53
54
55
56
57
58
59
60



Scheme 1. Scheme for the synthesis of AD-AN-AD.

Host-Guest Complexation Studies of AD-AN-AD and β -CD. Addition of two equivalents of β -CD to an aqueous solution of AD-AN-AD resulted in the formation of the bis-inclusion complex β -CD \subset AD-AN-AD \supset β -CD, in which the adamantane moieties of AD-AN-AD are encapsulated inside β -CD cavity, as shown in Scheme 2. Formation of the bis-inclusion complex was studied using isothermal titration calorimetry (ITC) and ^1H NMR spectroscopy.



Scheme 2. Formation of bis-inclusion complex β -CD \subset AD-AN-AD \supset β -CD.

Isothermal Titration Calorimetry. The ITC experiment was carried out by taking β -CD (10 mM, 40 μL) in the syringe and AD-AN-AD (0.1 mM, 200 μL) in the cell. Heat changes observed for AD-AN-AD/ β -CD complexation was moderately high. The raw data and fit are shown in Figure 2. The fit parameters obtained are: $K_a = (6.07 \pm 0.1) \times 10^3 \text{ M}^{-1}$, $\Delta H = -24.4 \pm 0.2 \text{ kJ mol}^{-1}$ and $\Delta S = -9.61 \text{ J mol}^{-1} \text{ K}^{-1}$ and $n = 1.93$. The value of n (~ 2) indicates that AD-AN-AD has two binding sites for β -CD. Thus, ITC studies confirmed that a 1:2 complex is formed between the two as shown in Scheme 2. The K_a value obtained in this case is somewhat lower compared to the previous systems studied by us^{49, 53-56} and others.⁵⁷⁻⁵⁸ This is attributed to the presence of positively charged $-\text{NH}_2^+$ moieties close to the AD groups in AD-AN-AD. It is reported that K_a for the formation of 1-adamantane ammonium chloride (ADAC)/ β -CD complex is less compared to several other adamantane/ β -CD systems.⁵⁹⁻⁶⁰ This is explained to be due to shallow penetration of the AD moiety in ADAC in the β -CD cavity, leaving the ammonium terminus projecting above the wider rim.⁵⁹ In this configuration the ammonium head group

is better solvated and a considerable percentage of the cavity near the narrow rim will remain unoccupied.

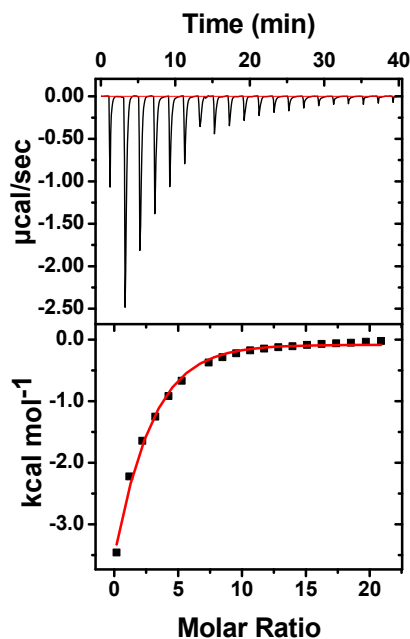


Figure 2. The ITC titration curve and fit obtained for the titration of β -CD with AD-AN-AD.

^1H NMR titration studies. ^1H NMR spectra of AD-AN-AD in the presence of varying amounts of β -CD, where the β -CD concentration changed from 0 – 2 equivalents, are shown in Figure 3a. Assignments of the various protons based on literature reports^{49, 61} are also shown in Figure 3a. In Figure 3a the dotted vertical lines indicate the original peak positions and the changes in peak positions are indicated by arrows in the top panel. The AD protons are labeled H_a (6H), H_b (3H) and H_c (6H). In the absence of β -CD, the H_a protons appeared as doublet of doublet at δ 1.84 ppm, H_c and H_b protons appeared as singlets at δ 2.25 and 2.35 ppm, respectively.⁴⁹ When inclusion of AD occurs, the H_a and H_b protons will be deeply inserted into the cavity and the H_c protons will remain close to the wider rim of β -CD. The inclusion process affects the signals due to all these protons. The doublet of doublet pattern of H_a changed into a broad singlet and shifted down field to δ 1.95 ppm. Signal due to H_b down-shifted to δ 2.55 ppm and H_c protons down-shifted to δ 2.39 ppm along with broadening, clearly providing evidence for inclusion of the AD moieties in the β -CD cavity.

1 Presence of a guest molecule in the CD cavity can also be confirmed by monitoring the changes
2
3 in the chemical shifts of CD protons. The H-3, H-5 and one of the H-6 protons of β -CD are directed
4
5 towards the interior of the cavity and the H-2, H-4 and one H-6 protons are on the outside (Figure S6, S.
6
7 I.). Presence of a guest inside the cavity affects the chemical shifts of all these protons, but signals of the
8
9 inside protons are affected more. The bottom panel in Figure 3b shows ^1H NMR signals for H-2 – H-6
10
11 protons of β -CD^{56,57} and the other panels show the shifts of these signals upon addition of AD-AN-AD
12
13 (0.5, 1.0 and 2.0 eq. of AD-AN-AD w.r.t. β -CD). The figure shows that addition of AD-AN-AD lead to
14
15 moderate upfield shifts for H-3 and H-5 protons and downfield shifts for H-2 and H-6 protons. The H-4
16
17 signal is not affected much. The H-2 proton is placed at the wider rim of the CD and in this case H-2 is
18
19 also affected because penetration of the AD moiety into the CD cavity is very shallow and part of this
20
21 moiety projects outside the wider rim (vide supra). Based on the NMR chemical shifts discussed so far
22
23 and the 1:2 stoichiometry derived from the ITC experiments, the structure of the inclusion complex can
24
25 be written as in Scheme 2, with both the AD moieties included in the β -CD cavities and the AN unit
26
27 placed in between the CDs. Since there are $-\text{NH}_2^+$ groups, which are highly hydrated on either side of
28
29 the AN moiety, we assume that AN is fully exposed to water. If this is the case, the AN protons should
30
31 not be affected by the presence of β -CD.
32
33
34
35
36
37
38

39 We, however, observed that in the presence of β -CD, the AN protons also exhibited chemical
40
41 shift changes. The H_e and H_f protons of the AN appeared as multiplets in the absence of β -CD (A
42
43 multiplet pattern is observed for these protons in few 9,10-dimethylene-substituted anthracene
44
45 derivatives.⁶² In order to confirm the assignments we obtained the single crystal X-ray structure of **3**
46
47 (which is the precursor of AD-AN-AD, Scheme 1). The X-ray structure of **3** is presented in the
48
49 supporting information along with its ^1H NMR spectrum (Figure S1, S2), which also exhibited multiplet
50
51 patterns for H_e and H_f). Up on addition of β -CD, the H_e and H_f protons of AD-AN-AD coalesced into
52
53 broad singlets and shifted down field (inset in Figure 3a), although these protons are away from the site
54
55
56
57
58
59
60

10

of inclusion (Scheme 2). The H_a protons (CH_2 protons linked to 9- and 10- positions of anthracene) also exhibited considerable down field shifts from δ 5.33 to 5.45 ppm. These NMR shifts have prompted us to consider other probable structures shown in Figure S7, for the AD-AN-AD/ β -CD complex.

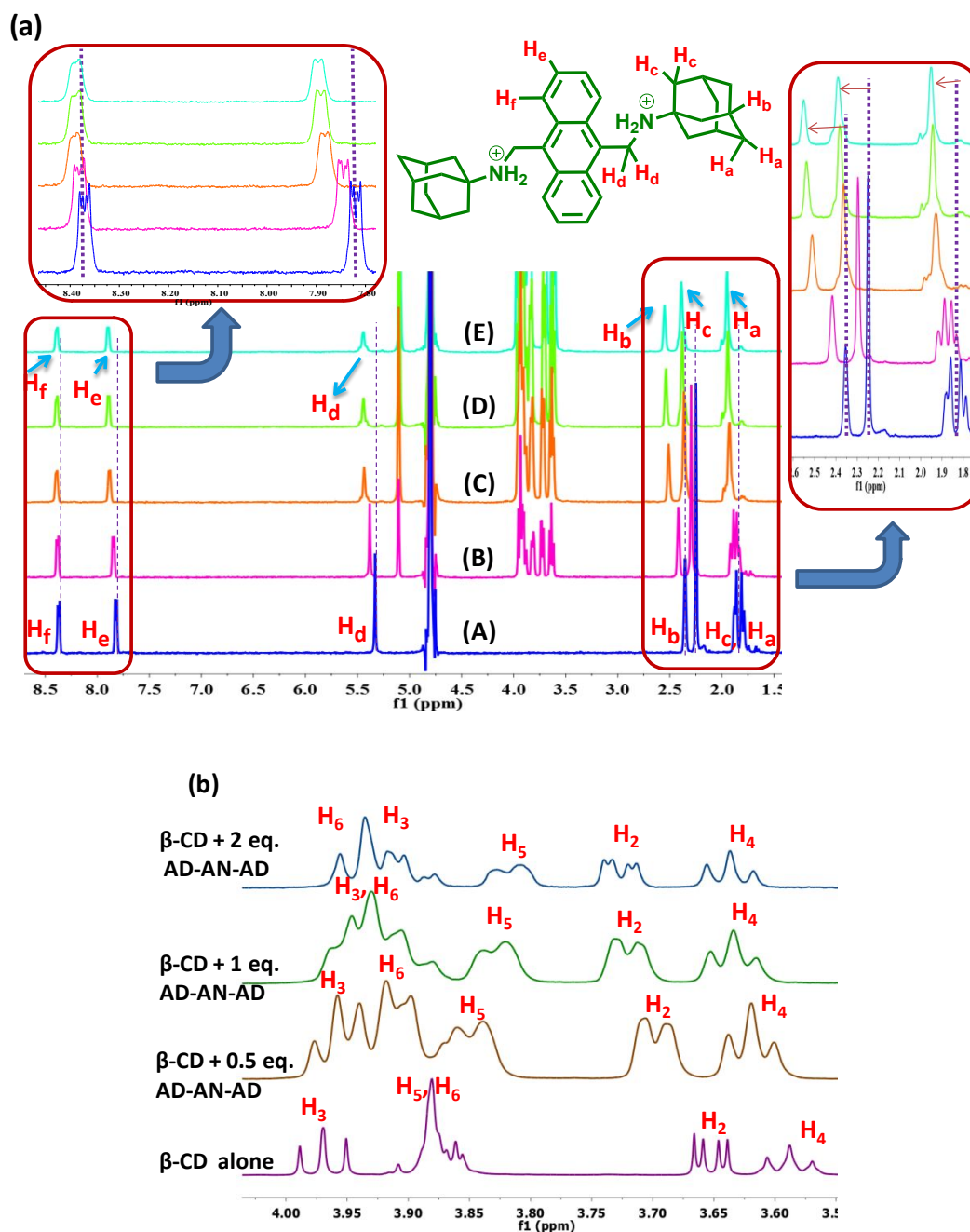


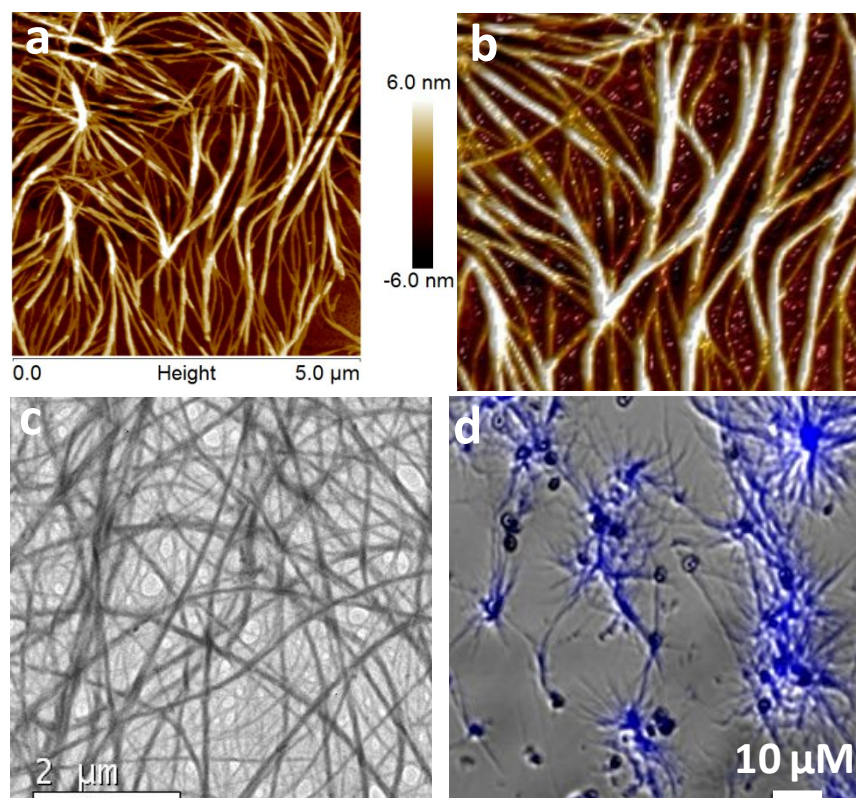
Figure 3. (a) 1H NMR spectra of AD-AN-AD (1 mM) in the absence (A) and presence (B-E) of β -CD (0.5 – 2 eq.) in D_2O . The insets show the shift of adamantyl and aromatic protons. (b) Selected area 1H NMR spectra showing changes in β -CD (0.5 mM) protons as [AD-AN-AD] is varied.

K_a value for anthracene/ β -CD inclusion complexation is $2.04 \times 10^3 \text{ M}^{-1}$.⁶³ In the case of AD-AN-AD the anthracene unit cannot be fully included in the cavity as its 9- and 10- positions are substituted by bulky groups. The AN moiety, however, can be partially included as shown in Figure S7a, where the terminal benzene rings of AN are included in β -CD. In this case the relevant K_a is that for benzene/ β -CD interaction, for which the value is only 170 M^{-1} .⁶³ The K_a value for adamantane/ β -CD interaction is $>10^4 \text{ M}^{-1}$.⁶³ Hence if the binding stoichiometry is 1:2, inclusion of AD moiety as shown in Scheme 2 is highly favored over Figure S7a. Further, we have previously shown that even partial inclusion of anthracene in β -CD will lead to changes in the absorption and emission profiles of the molecule.⁶⁴ We have observed that the photophysical properties of AD-AN-AD are unaffected by complexation with β -CD (vide infra). Because of these reasons the 1:2 and 1:4 complexes shown in Figure S7a,b can be ruled out. In addition, these structures also cannot explain the NMR shift observed for the H_d protons, as the molecular dimensions of β -CD will not allow entry of these protons into the cavity.

In the case of the β -CD \subset AD-AD \supset β -CD system reported previously by us, we observed chemical shift changes for protons that are placed much away from the site of inclusion binding.⁴⁹ These changes were attributed to secondary interactions leading to the formation of vesicles. The finding here is similar to that observed for the β -CD \subset AD-AD \supset β -CD system, and accordingly we attribute these changes to secondary interactions of the bis-inclusion complex. In order to probe whether such secondary interactions are taking place in the present system, we have subjected the β -CD/AD-AN-AD system to microscopic investigations.

Microscopic Studies. Aqueous solution of the bis-inclusion complex β -CD \subset AD-AN-AD \supset β -CD, prepared by mixing AD-AN-AD ($1 \times 10^{-5} \text{ M}$) and β -CD ($2 \times 10^{-5} \text{ M}$) was drop-casted onto freshly cleaved mica and air-dried for AFM analysis. The same aqueous solution was drop-casted on carbon-coated copper grid for TEM imaging. AFM and TEM images displayed largely interwoven fibrous

1 structures (Figure 4, see Figures S8 and S9, S.I. also). The TEM images showed highly rigid fibers
2 exhibiting fairly uniform width ranging from 50-200 nm and length reaching several micrometers. The
3
4 SAED pattern obtained in the TEM showed small spots in a ring pattern, suggesting that the fibers are
5 polycrystalline in nature (Figure S8c, S.I.). AFM images also showed nano-fibers of several
6 micrometers length and 50-150 nm width, which is in good agreement with the results obtained from
7 TEM experiments. The AFM height images suggested that these fibers have heights varying in a small
8 range of 4-8 nm. The AFM 3D image was also obtained for better visualization of rigidity of fibers,
9 which is shown in Figure 4b. The confocal laser scanning microscopy (CLSM) images of the fibers
10 (Figure 4d) showed fluorescent fibers indicating that the fluorescent anthracene moiety is incorporated
11 into the fibers.
12
13
14
15
16
17
18
19
20
21
22
23



51 Figure 4. (a) AFM height, (b) AFM 3-D, and (c) TEM images of AD-AN-AD (10^{-5} M)/ β -CD (2×10^{-5}
52 M) system in water. The (d) CLSM image of fluorescent nanofibers drop cast from AD-AN-AD (10^{-3}
53 M) and β -CD (2×10^{-3} M) aqueous solution.
54
55
56
57
58
59
60

Wide Angle X-ray Scattering (WAXS) Studies. The microscopic experiments suggested that the bis-inclusion complex $\beta\text{-CD}\subset\text{AD-AN-AD}\supset\beta\text{-CD}$ self-assembled into long fibrous structures. In order to understand the molecular level packing of the bis-inclusion complex $\beta\text{-CD}\subset\text{AD-AN-AD}\supset\beta\text{-CD}$ within the assembly, we carried out the WAXS studies on a dried film and the pattern obtained is shown in Figure 5 (the corresponding 2D plot is shown in the inset). The WAXS pattern showed several distinct X-ray scattering peaks, thereby suggesting that the observed fibers are highly crystalline.⁶⁵ We propose that scattering from different planes of self-assembled nano-fibers occurred to yield the observed multiple peak pattern. Among these, we could identify scattering peaks at 2θ of 5.83° and 11.02° which correspond, respectively, to d values of 15.14 \AA and 7.89 \AA . These could be assigned to molecular dimensions of $\beta\text{-CD}$. Also, sharp scattering occurred at a 2θ angle of 8.9° ($d = 9.5 \text{ \AA}$) which corresponds to the molecular length of anthracene unit. We also could identify a set of four peaks in the 2θ range of $23.5^\circ - 26.07^\circ$ which correspond to d values of 3.8 \AA , 3.6 \AA , 3.47 \AA and 3.41 \AA .

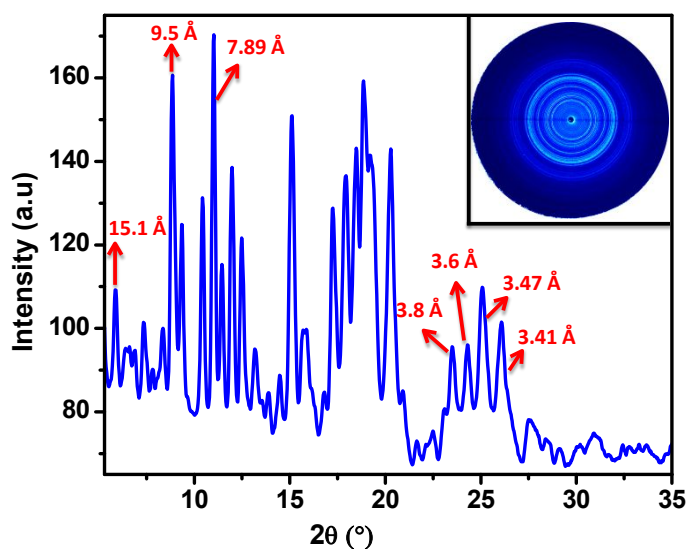


Figure 5. The WAXS pattern obtained for AD-AN-AD ($5 \times 10^{-4} \text{ M}$)/ $\beta\text{-CD}$ ($1 \times 10^{-3} \text{ M}$) self-assembled system with inset showing the corresponding 2D plot.

It is reported in the literature that the π -stacking of anthracene occurs at distances of $3.3 - 3.87 \text{ \AA}$,⁶⁵ and hence we assign these peaks to π - π stacking of the anthracene core of $\beta\text{-CD}\subset\text{AD-AN-AD}\supset\beta\text{-CD}$.

1 CD. We believe that the tendency of the anthracene core for π -stacking in the aqueous medium drives
2
3
4 the self-assembly of $\beta\text{-CD}\subset\text{AD-AN-AD}\supset\beta\text{-CD}$ into the fiber system. Thus the WAXS experiment
5
6 confirmed the crystalline nature of nanofibers which is in agreement with the crystalline morphology
7
8 obtained by TEM and AFM experiments.
9

10 **Self-Assembly of $\beta\text{-CD}\subset\text{AD-AN-AD}\supset\beta\text{-CD}$.** The bis-inclusion complex $\beta\text{-CD}\subset\text{AD-AN-}$
11
12 $\text{AD}\supset\beta\text{-CD}$ is a supramolecular bola-amphiphile with a hydrophobic and rigid anthracene at the core and
13
14 adamantane-included $\beta\text{-CD}$ moieties at both ends as shown in Scheme 2. The terminal groups are
15
16 hydrophilic due to the presence of the $\beta\text{-CD}$ s and positively charged ammonium groups attached to the
17
18 adamantane moieties. Self-assembly of the bis-inclusion complex into the long fibers most probably has
19
20 its origin in the tendency for the anthracene core for aggregation in the aqueous environment.
21
22 Aggregates are classified as J-aggregates when the absorption spectrum is red-shifted with respect to the
23
24 monomer peak, and H-aggregate when it is blue shifted.⁶⁷⁻⁶⁸ H-aggregates are generally non-emissive
25
26 but J-aggregates emit with enhanced rates. In order to see if any H- or J-aggregates were formed in the
27
28 AD-AN-AD/ $\beta\text{-CD}$ system the photophysical properties of this system were investigated. Figure 6 shows
29
30 the absorption and emission spectra of AD-AN-AD in the absence and presence of two equivalents of $\beta\text{-}$
31
32 CD. The inset of Figure 6 shows the fluorescence decay profiles of AD-AN-AD in the absence and
33
34 presence of $\beta\text{-CD}$. From Figure 6 it is clear that formation of the bis-inclusion complex and further self-
35
36 assembly into the fibrous networks had no influence on the absorption and emission properties of AD-
37
38 AN-AD. These results, in turn, ruled out the possibility of H- and J-aggregate formation in the AD-AN-
39
40 AD/ $\beta\text{-CD}$ system. As mentioned previously, this also ruled out the possibility of full or partial inclusion
41
42 of the AN moiety in the CD cavity.
43
44
45
46
47
48
49
50
51
52
53
54
55
56
57
58
59
60

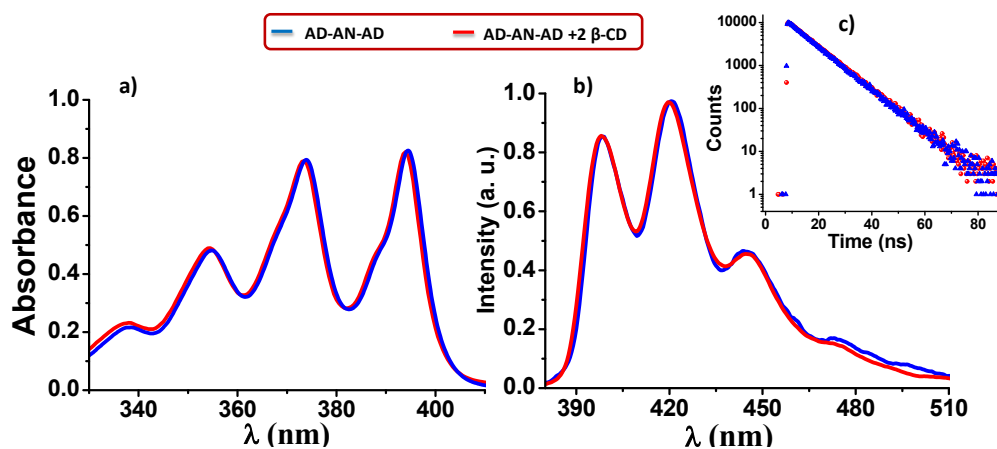


Figure 6. Absorption (a) and emission (b) spectra of AD-AN-AD in the absence (blue trace) and presence (red trace) of 2 eq. of β -CD. For the absorption spectra $[\text{AD-AN-AD}]$ was 8×10^{-5} M, and for (b) OD at the excitation wavelength (354 nm) was 0.06. Inset (c) shows the corresponding fluorescence decay profiles monitored at 420 nm.

According to Kasha, H-aggregates arise when molecules stack with their transition moments parallel and side-by-side and J-aggregation takes place when the transition dipoles are oriented head-to-tail.⁶⁷⁻⁶⁸ A closer look at the molecular dimensions of $\beta\text{-CD}\text{-AD-AN-AD}\text{-}\beta\text{-CD}$ (see Figure S10, S.I.), would reveal that this complex cannot form H- or J-aggregates because of geometrical restrictions. The edge-to-edge distance in $\beta\text{-CD}\text{-AD-AN-AD}\text{-}\beta\text{-CD}$ is ~ 2.6 nm. The outer diameter of β -CD is ~ 1.5 nm and the edge-to-edge distance in anthracene is ~ 0.97 nm, as shown in Figure S10 (S.I.). The large size of the β -CD compared to anthracene does not allow close packing of $\beta\text{-CD}\text{-AD-AN-AD}\text{-}\beta\text{-CD}$ into H- or J- aggregates. Given the molecular dimensions in Figure S10, the probable molecular stacking in H- and J-aggregates would be as shown in Figure S11a,b (S.I.). In the H-aggregate, the anthracene groups are π -stacked vertically one over another. Since the outer diameter of β -CD at the wider rim is 1.5 nm, the separation between adjacent anthracene residues will also be ~ 1.5 nm, if we assume that these residues are placed along the central plane of the β -CD. At this distance π -stacking interaction is not possible. In the J-aggregate shown, the anthracene chromophores are stacked in a head-to-tail fashion.

Using the molecular dimensions in Figure S10 (S.I.), we propose that the distance between the edge hydrogens of adjacent anthracene groups is ~ 5 Å. The π -clouds of the anthracene rings are also far apart to have any interaction. Thus, Figure S11 shows that geometrical restrictions do not allow formation of H- or J-aggregates of $\beta\text{-CD}\text{-AD-AN-AD}\beta\text{-CD}$.

Kasha proposed H- and J- aggregation based on the spatial dependence of the Coulombic coupling between the monomers.⁶⁷ Spano and co-workers recently pointed out that, in addition to long range Coulombic coupling, short range charge transfer (CT) mediated interactions must also be considered in molecular aggregates.⁶⁹⁻⁷⁰ Since Coulombic and CT-mediated couplings exist simultaneously in tightly packed molecular aggregates, the interference between these two interactions must be considered when defining J- and H- aggregates. Spano's group recently put forward the concept of "null" aggregates where the Coulomb and CT couplings destructively interfere and effectively cancel out. Such systems will have spectroscopic properties closely resembling those of unaggregated molecules in solution.⁶⁹ Null aggregation arises due to translational displacements ("slips") and twists between neighboring chromophores which influences the short range interaction severely.

The first example of null-aggregate is recently reported by Würthner and co-workers in the case of bis(perylene bisimide) (PBI) foldamers in which two PBI chromophores are covalently linked in the bay position by spacer moieties of different length and steric demand.⁷¹ The authors claimed that one of the foldamers, where the torsional angle (α) between the foldamers is 25° and the centers of the chromophores is displaced by 2.1 Å, exhibited properties characteristic of null-aggregates as demanded by Spano's theory. Very recently, Hariharan and co-workers have reported a novel Greek cross (+) assembly ($\alpha = 90^\circ$) of 1,7-dibromoperylene-3,4,9,10-tetracarboxylic tetrabutyl ester (PTE-Br₂), which exhibited null exciton coupling-mediated monomer-like optical characteristics in the crystalline state.⁷²

We propose that the fiber networks formed in the AD-AN-AD/ β -CD solution are null-aggregates of $\beta\text{-CD}\text{-AD-AN-AD}\beta\text{-CD}$. Our proposal is based on the molecular stacking observed for **3**, which is

1 the precursor of AD-AN-AD. **3** has bulky adamantane groups on either side and stacks in such a way to
2 avoid steric interactions between adamantane groups, as shown by the molecular packing in the crystals
3 (Figure 7). The anthracene groups are stacked in parallel planes with their long axis rotated by 56.06°
4 with respect to the preceding and succeeding neighbors. The rotation angle is close to the magic angle of
5 54.7° . Average π - π stacking distance in the assembly is 3.64 \AA , which is the value normally observed
6 for aromatic π -stacked systems.⁶⁶ The molecular packing in **3** also provides us with a strategy for the
7 design of null aggregates. Planar chromophores such as anthracene can be substituted with bulky
8 adamantane moieties so that the molecules can pack in the crystals only in the crisscross manner
9 exhibited in the case of **3**.

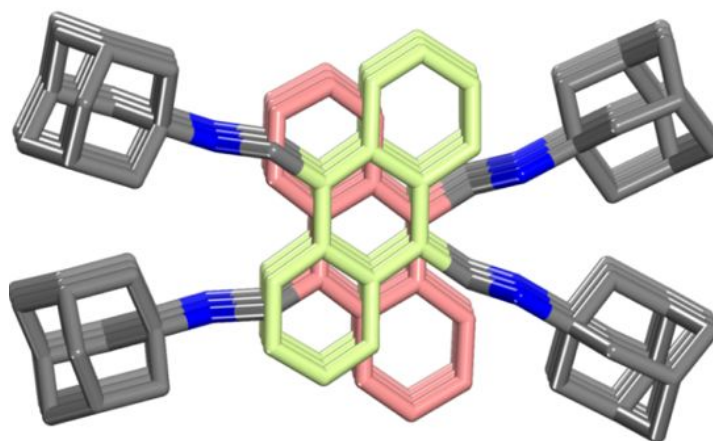
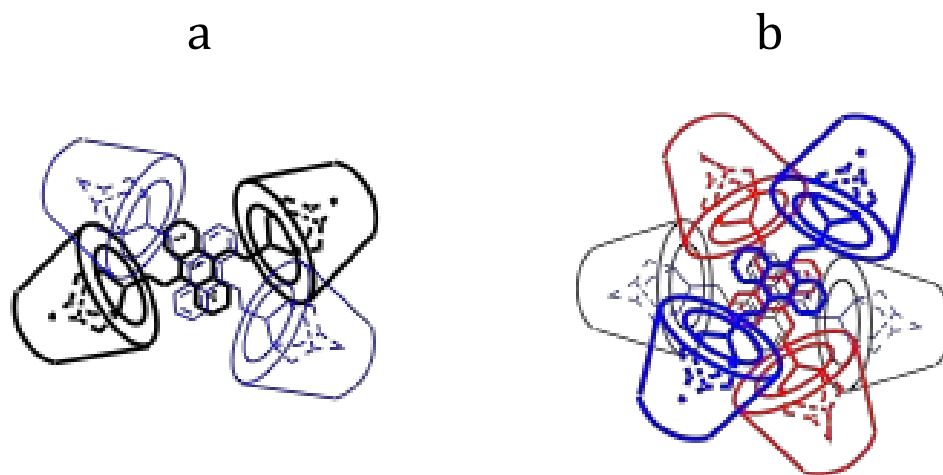


Figure 7. Molecular packing in the crystals of **3**.

10 If the stacking in $\beta\text{-CD}\leftarrow\text{AD-AN-AD}\rightarrow\beta\text{-CD}$ is same as in **3**, $\beta\text{-CD}\leftarrow\text{AD-AN-AD}\rightarrow\beta\text{-CD}$ will
11 stack as shown in Figure 8a. The third stack will be exactly over the first one. The center-to-center
12 distance between AD groups in the first and third stacks is 7.28 \AA in Figure 7. When the AD groups are
13 replaced by $\beta\text{-CD}$, a center-to-center distance of 15.3 \AA would be required between the first and third
14 layers to stack one $\beta\text{-CD}$ over another $\beta\text{-CD}$. If this is the case there will not be any π - π stacking
15 interaction as the anthracene groups in successive stacks would be separated by about 7.65 \AA . In order
16
17
18
19
20
21
22
23
24
25
26
27
28
29
30
31
32
33
34
35
36
37
38
39
40
41
42
43
44
45
46
47
48
49
50
51
52
53
54
55
56
57
58
59
60

1 to keep the π -stacking distance at 3.6 Å and to accommodate the steric bulk of the β -CD groups, the β -
2 CD-AD-AN-AD- β -CD molecules in successive layers will be twisted such that β -CD molecules in
3
4
5
6 one stack will come above another β -CD only in the fifth or sixth stack, meaning that there will be a
7
8 twist angle of $60 - 72^\circ$ between β -CD-AD-AN-AD- β -CD molecules in successive stacks. A probable
9
10 schematic of the assembly is shown in Figure 8b.



11
12
13
14
15
16
17
18
19
20
21
22
23
24
25
26
27
28
29
30 Figure 8. Probable stacking modes of β -CD-AD-AN-AD- β -CD in the fiber networks (The nitrogen
31 atoms are not shown).
32
33
34

35 Several authors have reported cross-dipole stacks of aromatic chromophores where the twist
36 angle α varied from 0 to 90° .⁷²⁻⁷⁵ In these systems non-zero exciton coupling leads to perturbations in
37 the spectroscopic properties. For example, a PTE system reported by Hariharan and co-workers
38 exhibited red shifts in the absorption and emission spectra compared to the monomer when $\alpha = 70.2^\circ$.⁷²
39 Ma et al also reported small red shifts in the absorption and emission spectra for a system where $\alpha =$
40 62° .⁷⁵ In the present case we propose that the anthracene chromophores are twisted in the range of 60-
41 72° as shown in Figure 8b, and this does not lead to any perturbation in the spectroscopic properties. In
42 other words, these aggregates exhibit properties of null aggregates in the proposed twist angle.
43
44
45
46
47
48
49
50
51
52
53

54 In this study we have investigated only the β -CD complex of AD-AN-AD and proposed that the
55 larger size of β -CD compared to anthracene does not allow the type of packing observed for **3** (Figure
56
57
58
59
60

7). In this context, it may be important to investigate the behavior of α -CD and γ -CD complexes of AD-AN-AD. The outer diameter of α -CD is 13.7 Å at the wider rim and this may allow better packing of the AD-AN-AD/ α -CD bis-inclusion complex. Since γ -CD is larger, stacking of AD-AN-AD/ γ -CD bis-inclusion complex would be more difficult. Such considerations, however, have to take into account the lower stabilities of AD/ α -CD and AD/ γ -CD complexes. Cromwell et al. have studied the complexation of adamantane carboxylate with α -, β - and γ -CDs and found that complexation with β -CD is the most exergonic ($\Delta G^0 = -5.85 \text{ kcal mol}^{-1}$) and exothermic ($\Delta H^0 = -4.85 \text{ kcal mol}^{-1}$).⁵⁸ ΔG^0 for the binding of α -CD was 140-fold lower and binding with γ -CD was found to be endothermic. This study highlighted the importance of an optimum matching of the cavity size and guest size in determining the strength of binding. Since the strength of AD/ α -CD and AD/ γ -CD systems are very low, we may not observe the fiber-type assembly for AD-AN-AD/ α -CD or AD-AN-AD/ γ -CD systems.

If fibers are formed by stacking of bis-inclusion complexes as in Figure 8b, the outer diameter of the fiber would be around 2.6 nm (see Figure S10). The fibers observed in AFM have diameters in the 50-200 nm range. This suggest that the fibers are bundled together, which most probably would involve hydrogen bonding interactions between fibers. The fibers formed by stacking as shown in Figure 8b will have their outer surface covered by the narrow rims of β -CD. The narrow rim of β -CD is made up of seven primary hydroxyl groups which can readily form hydrogen bonds with solvent molecules or other fibers. Since there are large numbers of narrow rims on the outer surface of every fiber, large number of fibers can come together and get stabilized through hydrogen bonding to give the observed fiber network. We could not confirm the structure of the null aggregate by X-ray crystallography because β -CD \subset AD-AN-AD \supset β -CD did not crystallize from aqueous medium and formed the fiber networks even at very low concentrations ($\leq 10^{-5} \text{ M}$). The anthracene groups are buried inside the fibers and their outer surface is loaded with the narrow rims of β -CD having primary hydroxyl groups even in the bundled

1 state, which makes them highly hydrophilic. Thus, these fibers are soluble in water and do not form
2
3
4 gels.

5
6 The stacking modes presented in Figure 8b also explains the chemical shift changes observed in
7
8 the NMR titration experiment (Figure 3a). The π - π stacking distance in the assembly is $< 4 \text{ \AA}$, which
9
10 explains the observed chemical shift changes for the ring protons. The H_d protons are sandwiched
11
12 between aromatic rings and hence experience large shifts. The photophysical properties of the aggregate
13
14 and monomer are identical because the assembly is a null aggregate.
15
16
17
18

19 4. CONCLUSIONS

20
21
22 The bis-adamantane derivative of anthracene, AD-AN-AD, where the adamantane groups are connected
23
24 to the 9- and 10- positions of anthracene through a short linker, readily formed a bis-inclusion complex
25
26 in aqueous solution, in the presence of two equivalents of β -CD. The bis-inclusion complex, β -CD \subset AD-
27
28 AN-AD \supset β -CD, which is a bola-amphiphile, spontaneously self-assembled in to a nanofiber network.
29
30 Images of the nanofiber assemblies were obtained in AFM, TEM and CLSM experiments. The
31
32 nanofibers were highly crystalline as confirmed from WAXS studies. We presumed that tight packing of
33
34 the anthracene moieties in β -CD \subset AD-AN-AD \supset β -CD into a crystalline aggregate is responsible for the
35
36 crystallinity of the fibers. We proposed that β -CD \subset AD-AN-AD \supset β -CD tightly packed into null
37
38 aggregates where the stacking distance between anthracene molecules is $\sim 3.6 \text{ \AA}$ and the long axis of
39
40 anthracene in one stack is rotated in the range of 60 - 72° with respect to anthracenes in the preceding and
41
42 succeeding layers. The null aggregate can stack together to give the observed 1-D fiber networks.
43
44 Photophysical properties of the fiber system were identical to those of the monomer units, and this is in
45
46 conformity with the definition of null aggregate. The proposal of the null aggregate is based on the
47
48 observed crystal packing in the precursor of AD-AN-AD, where the molecules stacks in a crisscross
49
50 fashion to avoid steric crowding. In this mode of stacking the stacking distance is 3.64 \AA and the
51
52
53
54
55
56
57
58
59
60

1 crisscross angle $\alpha = 56.06^\circ$. In short, this study also provides a simple and effective strategy for
2
3
4 designing null aggregates of planar chromophores in solution and solid state.
5
6
7

8 **ASSOCIATED CONTENT**

10 **Supporting Information.**

11
12
13 Synthesis, ^1H , ^{13}C NMR and ESI-HRMS of AD-AN-AD, Single crystal structure of molecule 3 (in
14
15 scheme 1), Molecular dimensions of $\beta\text{-CD}\subset\text{AD-AN-AD}\supset\beta\text{-CD}$ complex, Additional TEM, AFM
16
17 images nanofibers. This material is available free of charge via the Internet at <http://pubs.acs.org>
18
19
20
21
22
23

24 **AUTHOR INFORMATION**

26 **Corresponding Author**

27
28
29 * E-mail: gopidaskr@gmail.com
30
31

32 **Present Addresses**

33
34
35 Dr. Nagaraj Nayak
36

37 Department of Chemistry, Indian Institute of Technology-Bombay, Powai, Mumbai – 400 076 (India)
38
39
40

41 **ACKNOWLEDGEMENTS**

42
43
44
45 We thank CSIR, Government of India (project no. HCP0012) for financial support. We are also
46
47 thankful to Dr. Sunil Varughese for single crystal X-ray analysis, Mr. Kiran Mohan for TEM and Mr.
48
49 Aswin Maheswar for AFM analysis. K.R.G. thanks CSIR for Emeritus scheme and N. N. thanks CSIR
50
51 for a research fellowship.
52
53
54
55
56
57
58
59
60

1
2
3
4
5
6
7
8
9
10
11
12
13
14
15
16
17
18
19
20
21
22
23
24
25
26
27
28
29
30
31
32
33
34
35
36
37
38
39
40
41
42
43
44
45
46
47
48
49
50
51
52
53
54
55
56
57
58
59
60
REFERENCES

- (1) Jürgen-Hinrich, F.; Tianyu, W. Bolaamphiphiles. *Chem. Rev.* **2004**, *104*, 2901-2938.
- (2) Zhang, X.; Wang, C. Supramolecular amphiphiles. *Chem. Soc. Rev.* **2011**, *40* (1), 94-101.
- (3) Ávalos, M.; Babiano, R.; Cintas, P.; Gómez-Carretero, A.; Jiménez, J. L.; Lozano, M.; Ortiz, A. L.; Palacios, J. C.; Pinazo, A. A family of hydrogels based on ureido-linked aminopolyol-derived amphiphiles and bolaamphiphiles: synthesis, gelation under thermal and sonochemical stimuli, and mesomorphic characterization. *Chem. Eur. J.* **2008**, *14* (18), 5656-5669.
- (4) Dhasaiyan, P.; Prasad, B. L. V. Self-assembly of bolaamphiphilic molecules. *Chem. Rec.* **2017**, *17* (6), 597-610.
- (5) Sorrenti, A.; Illa, O.; Ortuno, R. M. Amphiphiles in aqueous solution: well beyond a soap bubble. *Chem. Soc. Rev.* **2013**, *42* (21), 8200-19.
- (6) Amit, M.; Yuran, S.; Gazit, E.; Reches, M.; Ashkenasy, N. Tailor-made functional peptide self-assembling nanostructures. *Adv. Mater.* **2018**, *30* (41), 1707083.
- (7) Zhu, X.; Liu, M. Self-assembly and morphology control of new L-glutamic acid-based amphiphilic random copolymers: giant vesicles, vesicles, spheres, and honeycomb film. *Langmuir* **2011**, *27* (21), 12844-12850.
- (8) Gerber, S.; Garamus, V. M.; Milkereit, G.; Vill, V. Mixed micelles formed by SDS and a bolaamphiphile with carbohydrate headgroups. *Langmuir* **2005**, *21* (15), 6707-6711.
- (9) Wang, G.; Wang, C.; Wang, Z.; Zhang, X. Bolaform superamphiphile based on a dynamic covalent bond and its self-assembly in water. *Langmuir* **2011**, *27* (20), 12375-12380.
- (10) Buerkle, L.; Rowan, S. Supramolecular gels formed from multi-component low molecular weight species. *Chem. Soc. Rev.* **2012**, *41* (18), 6089-6102.
- (11) Du, X.; Zhou, J.; Shi, J.; Xu, B. Supramolecular hydrogelators and hydrogels: from soft matter to molecular biomaterials. *Chem. Rev.* **2015**, *115* (24), 13165-13307.

- (12) Meng, Y.; Jiang, J.; Liu, M. Self-assembled nanohelix from a bolaamphiphilic diacetylene via hydrogelation and selective responsiveness towards amino acids and nucleobases. *Nanoscale* **2017**, *9* (21), 7199-7206.
- (13) Cui, H.; Webber, M. J.; Stupp, S. I. Self-assembly of peptide amphiphiles: from molecules to nanostructures to biomaterials. *Peptide Science* **2010**, *94* (1), 1-18.
- (14) Kumar, N. S. S.; Shinto, V.; Gopinathan, N.; Suresh, D. Hierarchical self-Assembly of donor-acceptor-substituted butadiene amphiphiles into photoresponsive vesicles and gels. *Angew. Chem. Int. Ed.* **2006**, *118*, 6317-6321.
- (15) Denisov, I. G.; Sligar, S. G. Nanodiscs in membrane biochemistry and biophysics. *Chem. Rev.* **2017**, *117* (6), 4669-4713.
- (16) Yasuhara, K.; Arakida, J.; Ravula, T.; Ramadugu, S. K.; Sahoo, B.; Kikuchi, J.-i.; Ramamoorthy, A. Spontaneous lipid nanodisc formation by amphiphilic polymethacrylate copolymers. *J. Am. Chem. Soc.* **2017**, *139* (51), 18657-18663.
- (17) Bayburt, T. H.; Sligar, S. G. Membrane protein assembly into nanodiscs. *FEBS Lett.* **2010**, *584* (9), 1721-1727.
- (18) Ravula, T.; Hardin, N. Z.; Ramadugu, S. K.; Cox, S. J.; Ramamoorthy, A. Formation of pH-resistant monodispersed polymer-lipid nanodiscs. *Angew. Chem. Int. Ed.* **2018**, *57* (5), 1342-1345.
- (19) Antonietti, M.; Förster, S. Vesicles and liposomes: a self-assembly principle beyond lipids. *Adv. Mater.* **2003**, *15* (16), 1323-1333.
- (20) Falvey, P.; Lim, C. W.; Darcy, R.; Revermann, T.; Karst, U.; Giesbers, M.; Marcelis, A. T.; Lazar, A.; Coleman, A. W.; Reinhoudt, D. N.; Ravoo, B. J. Bilayer vesicles of amphiphilic cyclodextrins: host membranes that recognize guest molecules. *Chem. Eur. J.* **2005**, *11* (4), 1171-1180.
- (21) Felici, M.; Marza-Perez, M.; Hatzakis, N. S.; Nolte, R. J.; Feiters, M. C. Beta-cyclodextrin-appended giant amphiphile: aggregation to vesicle polymersomes and immobilisation of enzymes. *Chem. Eur. J.* **2008**, *14* (32), 9914-9920.

- (22) Sun, T.; Yan, H.; Liu, G.; Hao, J.; Su, J.; Li, S.; Xing, P.; Hao, A. Strategy of directly employing paclitaxel to construct vesicles. *J. Phys. Chem. B* **2012**, *116* (50), 14628-14636.
- (23) Jiao, D.; Geng, J.; Loh, X.; Das, D.; Lee, T.-C.; Scherman, O. Supramolecular peptide amphiphile vesicles through host-guest complexation. *Angew. Chem. Int. Ed.* **2012**, *51* (38), 9633-9637.
- (24) Guo, D. S.; Wang, K.; Wang, Y. X.; Liu, Y. Cholinesterase-responsive supramolecular vesicle. *J. Am. Chem. Soc.* **2012**, *134* (24), 10244-10250.
- (25) Landsmann, S.; Luka, M.; Polarz, S. Bolaform surfactants with polyoxometalate head groups and their assembly into ultra-small monolayer membrane vesicles. *Nature Commun.* **2012**, *3*, 1299.
- (26) Ajayaghosh, A.; Varghese, R.; Mahesh, S.; Praveen, V. From vesicles to helical nanotubes: a sergeant-and-soldiers effect in the self-assembly of oligo(p-phenyleneethynylene)s. *Angew. Chem. Int. Ed.* **2006**, *45* (46), 7729-7732.
- (27) Wang, T.; Jiang, J.; Liu, Y.; Li, Z.; Liu, M. Hierarchical self-assembly of bolaamphiphiles with a hybrid spacer and L-glutamic acid headgroup: pH- and surface-triggered hydrogels, vesicles, nanofibers, and nanotubes. *Langmuir* **2010**, *26* (24), 18694-18700.
- (28) Shimizu, T.; Kameta, N.; Ding, W.; Masuda, M. Supramolecular self-assembly into biofunctional soft nanotubes: from bilayers to monolayers. *Langmuir* **2016**, *32* (47), 12242-12264.
- (29) Zhan, C.; Gao, P.; Liu, M. Self-assembled helical spherical-nanotubes from an L-glutamic acid based bolaamphiphilic low molecular mass organogelator. *Chem. Commun.* **2005**, (4), 462-464.
- (30) Kameta, N.; Dong, J.; Yui, H. Thermoresponsive PEG-coated nanotubes as chiral selectors of amino acids and peptides. *Small* **2018**, *14* (15), 1800030.
- (31) Wang, C.; Yin, S.; Chen, S.; Xu, H.; Wang, Z.; Zhang, X. Controlled self-assembly manipulated by charge-transfer interactions: from tubes to vesicles. *Angew. Chem. Int. Ed.* **2008**, *47* (47), 9049-9052.
- (32) Shao, H.; Seifert, J.; Romano, N. C.; Gao, M.; Helmus, J. J.; Jaroniec, C. P.; Modarelli, D. A.; Parquette, J. R. Amphiphilic self-assembly of an n-type nanotube. *Angew. Chem. Int. Ed.* **2010**, *49* (42), 7688-7691.

- (33) Yashima, E.; Ousaka, N.; Taura, D.; Shimomura, K.; Ikai, T.; Maeda, K. Supramolecular helical systems: helical assemblies of small molecules, foldamers, and polymers with chiral amplification and their functions. *Chem. Rev.* **2016**, *116* (22), 13752-13990.
- (34) Jeon, Y.; Bharadwaj, P.; Choi, S.; Lee, J.; Kim, K. Supramolecular amphiphiles: spontaneous formation of vesicles triggered by formation of a charge-transfer complex in a host. *Angew. Chem. Int. Ed.* **2002**, *41* (23), 4474-4476.
- (35) Wang, C.; Guo, Y.; Wang, Y.; Xu, H.; Wang, R.; Zhang, X. Supramolecular amphiphiles based on a water-soluble charge-transfer complex: fabrication of ultralong nanofibers with tunable straightness. *Angew. Chem. Int. Ed.* **2009**, *48* (47), 8962-8965.
- (36) Yu, G.; Jie, K.; Huang, F. Supramolecular amphiphiles based on host-guest molecular recognition motifs. *Chem. Rev.* **2015**, *115* (15), 7240-7303.
- (37) Jie, K.; Zhou, Y.; Yao, Y.; Huang, F. Macrocyclic amphiphiles. *Chem. Soc. Rev.* **2015**, *44* (11), 3568-3587.
- (38) Wang, C.; Wang, Z.; Zhang, X. Amphiphilic building blocks for self-assembly: from amphiphiles to supra-amphiphiles. *Acc. Chem. Res.* **2012**, *45* (4), 608-618.
- (39) Cao, Y.; Hu, X. Y.; Li, Y.; Zou, X.; Xiong, S.; Lin, C.; Shen, Y. Z.; Wang, L. Multistimuli-responsive supramolecular vesicles based on water-soluble pillar[6]arene and SAINT complexation for controllable drug release. *J. Am. Chem. Soc.* **2014**, *136* (30), 10762-10769.
- (40) Nayak, N.; Gopidas, K. R. Integrative self-sorting in a three component system leading to formation of long fibrous structures. *ChemistrySelect* **2016**, *5*, 1028-1032.
- (41) Tao, W.; Liu, Y.; Jiang, B.; Yu, S.; Huang, W.; Zhou, Y.; Yan, D. A linear-hyperbranched supramolecular amphiphile and its self-assembly into vesicles with great ductility. *J. Am. Chem. Soc.* **2012**, *134* (2), 762-764.

- (42) Zhang, H.; Liu, Z.; Xin, F.; An, W.; Hao, A.; Li, J.; Li, Y.; Sun, L.; Sun, T.; Zhao, W.; Li, Y.; Kong, L. Successively-responsive drug-carrier vesicles assembled by 'supramolecular amphiphiles'. *Carbohydr. Res.* **2011**, *346* (2), 294-304.
- (43) Harada, A.; Takashima, Y.; Nakahata, M. Supramolecular polymeric materials via cyclodextrin-guest interactions. *Acc. Chem. Res.* **2014**, *47* (7), 2128-2140.
- (44) Harada, A.; Takashima, Y.; Yamaguchi, H. Cyclodextrin-based supramolecular polymers. *Chem. Soc. Rev.* **2009**, *38* (4), 875-882.
- (45) Sun, T.; Li, Y.; Zhang, H.; Li, J.; Xin, F.; Kong, L.; Hao, A. pH-reversible vesicles based on the "supramolecular amphiphilicities" formed by cyclodextrin and anthraquinone derivate. *Colloids Surf. A* **2011**, *375* (1-3), 87-96.
- (46) Zhang, H.; Shen, J.; Liu, Z.; Hao, A.; Bai, Y.; An, W. Multi-responsive cyclodextrin vesicles assembled by 'supramolecular bola-amphiphiles'. *Supramol. Chem.* **2010**, *22* (5), 297-310.
- (47) Li, S.; Zhang, L.; Wang, B.; Ma, M.; Xing, P.; Chu, X.; Zhang, Y.; Hao, A. An easy approach for constructing vesicles by using aromatic molecules with β -cyclodextrin. *Soft Matter* **2015**, *11* (9), 1767-1777.
- (48) Rothenbühler, S.; Bösch, C. D.; Langenegger, S. M.; Liu, S.-X.; Häner, R. Self-assembly of a redox-active bolaamphiphile into supramolecular vesicles. *Org. Biomol. Chem.* **2018**, *16* (38), 6886-6889.
- (49) Nayak, N.; Gopidas, K. R. Unusual self-assembly of a hydrophilic β -cyclodextrin inclusion complex into vesicles capable of drug encapsulation and release. *J. Mater. Chem. B* **2015**, *3* (17), 3425-3428.
- (50) Sallas, F.; Darcy, R. Amphiphilic cyclodextrins – advances in synthesis and supramolecular chemistry. *Eur. J. Org. Chem.* **2008**, *2008* (6), 957-969.

- (51) Freyer, M. W.; Lewis, E. A. Isothermal titration calorimetry: experimental design, data analysis, and probing macromolecule/ligand binding and kinetic interactions. *Methods in Cell Biology*, Academic Press: 2008; Vol. 84, 79-113.
- (52) Sanju, K. S.; Ramaiah, D. White photoluminescence and electroluminescence from a ternary system in solution and a polymer matrix. *Chem. Commun.* **2013**, 49 (99), 11626-11628.
- (53) Krishnan, R.; Gopidas, K. R. Beta-cyclodextrin as an end-to-end connector. *J. Phys. Chem. Lett.* **2011**, 2, 2094–2098
- (54) Krishnan, S. B.; Gopidas, K. R. Supramolecular chirality in a hierarchically self-assembled mixed-stack charge-transfer complex. *Chem. Eur. J.* **2017**, 23 (40), 9600-9606.
- (55) Krishnan, R.; Krishnan, S. B.; Balan, B.; Gopidas, K. R. Self-assembly and photoinduced electron transfer in a donor- β -cyclodextrin-acceptor supramolecular system. *J. Chem. Sci.* **2018**, 130 (10), 134.
- (56) Krishnan, R.; Rakhi, A. M.; Gopidas, K. R. Study of β -cyclodextrin–pyromellitic diimide complexation: conformational analysis of binary and ternary complex structures by induced circular dichroism and 2D NMR spectroscopies. *J. Phys. Chem. C* **2012**, 116 (47), 25004-25014.
- (57) Carrazana, J.; Jover, A.; Meijide, F.; Soto, V. H.; Vazquez Tato, J. Complexation of adamantyl compounds by beta-cyclodextrin and monoaminoderivatives. *J. Phys. Chem. B* **2005**, 109 (19), 9719-9726.
- (58) Cromwell, W. C.; Bystrom, K.; Eftink, M. R. Cyclodextrin-adamantanecarboxyiate inclusion complexes: studies of the variation in cavity size. *J. Phys. Chem.* **1985**, 89 (2), 326-332.
- (59) Briggner, L. E.; Ni, X. R.; Tempesti, F.; Wadsö, I. Microcalorimetric titration of β -cyclodextrin with adamantane-1-carboxylate. *Thermochim. Acta* **1986**, 109 (1), 139-143.
- (60) Gelb, R.; Schwartz, L. Complexation of adamantane-ammonium substrates by beta-cyclodextrin and its O-methylated derivatives. *J. Incl. Phenom.* **1989**, 7 (5), 537-543.

- (61) Hasegawa, Y.; Miyauchi, M.; Takashima, Y.; Yamaguchi, H.; Harada, A. Supramolecular polymers formed from β -Cyclodextrins dimer linked by poly(ethylene glycol) and guest dimers. *Macromolecules* **2005**, *38* (9), 3724-3730.
- (62) Liu, W.; Wang, Y.; Sun, M.; Zhang, D.; Zheng, M.; Yang, W. Alkoxy-position effects on piezofluorochromism and aggregation-induced emission of 9,10-bis(alkoxystyryl)anthracenes. *Chem. Commun.* **2013**, *49* (54), 6042-6044.
- (63) Rekharsky, M. V.; Inoue, Y. Complexation thermodynamics of cyclodextrins. *Chem. Rev.* **1998**, *98* (5), 1875-1917.
- (64) Balan, B.; Gopidas, K. R. An anthracene-appended β -cyclodextrin-based dyad: study of self-assembly and photoinduced electron-transfer processes. *Chem. Eur. J.* **2007**, *13* (18), 5173-5185.
- (65) Shigemitsu, H.; Hisaki, I.; Kometani, E.; Yasumiya, D.; Sakamoto, Y.; Osaka, K.; Thakur, T. S.; Saeki, A.; Seki, S.; Kimura, F.; et al. Crystalline supramolecular nanofibers based on dehydrobenzoannulene derivatives. *Chem. Eur. J.* **2013**, *19* (45), 15366-15377.
- (66) Egbe, D. A. M.; Türk, S.; Rathgeber, S.; Kühnlenz, F.; Jadhav, R.; Wild, A.; Birckner, E.; Adam, G.; Pivrikas, A.; Cimrova, V.; Knör, G.; Sariciftci, N. S.; et al. Anthracene based conjugated polymers: correlation between π - π -stacking ability, photophysical properties, charge carrier mobility, and photovoltaic performance. *Macromolecules* **2010**, *43* (3), 1261-1269.
- (67) Kasha, M.; Rawls, H. R.; Ashraf El-Bayoumi, M. The exciton model in molecular spectroscopy. *Pure Appl. Chem.*, 1965; *11*, 371-392.
- (68) Kasha, M. Energy transfer mechanisms and the molecular exciton model for molecular aggregates. *Radiat. Res.* **1963**, *20* (1), 55-70.
- (69) Hestand, N. J.; Spano, F. C. Molecular aggregate photophysics beyond the Kasha model: novel design principles for organic materials. *Acc. Chem. Res.* **2017**, *50* (2), 341-350.

(70) Hestand, N. J.; Spano, F. C. Interference between coulombic and CT-mediated couplings in molecular aggregates: H- to J-aggregate transformation in perylene-based π -stacks. *J. Chem. Phys.* **2015**, *143* (24), 244707.

(71) Kaufmann, C.; Bialas, D.; Stolte, M.; Würthner, F. Discrete π -stacks of perylene bisimide dyes within folda-dimers: insight into long- and short-range exciton coupling. *J. Am. Chem. Soc.* **2018**, *140* (31), 9986-9995.

(72) Sebastian, E.; Philip, A. M.; Benny, A.; Hariharan, M. Null exciton splitting in chromophoric greek cross (+) aggregate. *Angew. Chem. Int. Ed.* **2018**, *57* (48), 15696-15701.

(73) Xie, Z.; Yang, B.; Li, F.; Cheng, G.; Liu, L.; Yang, G.; Xu, H.; Ye, L.; Hanif, M.; Liu, S.; Ma, D.; Ma, Y. Cross dipole stacking in the crystal of distyrylbenzene derivative: the approach toward high solid-state luminescence efficiency. *J. Am. Chem. Soc.* **2005**, *127* (41), 14152-14153.

(74) Rösch, U.; Yao, S.; Wortmann, R.; Würthner, F. Fluorescent H-aggregates of merocyanine dyes. *Angew. Chem. Int. Ed.* **2006**, *45* (42), 7026-7030.

(75) Ma, S.; Zhang, J.; Qian, J.; Chen, J.; Xu, B.; Tian, W. Efficient spontaneous and stimulated emission from 1,4-bis(2,2-diphenylvinyl)benzene single crystals with cross-dipole stacking. *Adv. Opt. Mat.* **2015**, *3* (6), 763-768.

Table of Contents Graphic

